International Journal of Multidisciplinary Research and Development

IJMRD 2015; 2(3): 322-326
www.allsubjectjournal.com
Impact factor: 3.672
Received: 28-02-2015
Accepted: 16-03-2015
E-ISSN: 2349-4182
P-ISSN: 2349-5979

Manoj Kumar
Research Scholar
Department of Chemistry,
Centre of Advanced Study,
Faculty of Science,
Banaras Hindu University,
Varanasi - 221005, U.P., India.

Bali Ram
Professor Department of Chemistry, Centre of Advanced Study, Faculty of Science, Banaras Hindu University, Varanasi - 221005, U.P., India.

Correspondence:
Bali Ram
Professor Department of Chemistry, Centre of Advanced Study, Faculty of Science, Banaras Hindu University, Varanasi - 221005, U.P, India.

Non-equilibrium thermodynamic studies on transport of aqueous aluminium nitrate solutions across cellulose acetate membrane

Manoj Kumar, Bali Ram

Abstract
Hydrodynamic and electro-osmotic permeability measurements of water and aqueous solutions of Al $(NO_3)_3.9H_2O$ in the concentration range of 10^{-4} M to 10^{-3} M have been made across cellulose acetate membrane. The data obtained have been used to determine the transport equation using the theory of non-equilibrium thermodynamics. Streaming current generated during the transport of various permeants was also measured and its dependence on pressure investigated. Phenomenological coefficients have been determined using the transport equation and Saxen's relationship verified. Zeta potentials have been evaluated using electro-osmotic permeability and membrane-permeant conductance data. It has been observed that hydrodynamic and electro-osmotic permeabilities depend linearly on applied pressure difference and potential difference respectively.

Keywords: Non-equilibrium thermodynamics, Electro-osmotic flux, Streaming potential and Zeta potential.

1. Introduction
Membrane technology can be used in a large number of separation processes like reverse osmosis, nanofiltration etc. Cellulose acetate (CA) membranes developed during 1960 [1, 2], are the first type of membranes being used in commercial reverse osmosis (RO) water desalination plants. CA membranes are less expensive, have a longer life, require less cleaning, and are much more resistant to chlorine, as compared to other types of RO membranes. It is a model membrane system, and non-ion selective in nature [3, 4, 5] which requires higher pressure than other types of membranes and allows more salt passage. CA membranes have good toughness, high hydrophilicity and relatively low cost, hence they have been widely used for many purposes like, microfiltration, ultrafiltration, reverse osmosis and gas separation [6, 7].
According to the theory of non-equilibrium thermodynamics of steady states [8, 9, 10] fluxes are coupled, which can be identified using thermodynamic principles. These fluxes obey linear phenomenological relations and a stable steady state. Non-equilibrium steady states can also be stable even when the phenomenological relations are nonlinear [11, 12, 13].
In the present article, we have studied the hydrodynamic, electro-osmotic transport of aqueous salts solutions of Al (NO3)3.9H2O through cellulose acetate membrane and the results have been analyzed on the basis of theory of non-equilibrium thermodynamics of irreversible processes. Streaming current generated during the transport of various permeants was also measured for verifying Saxen's relationship. The results obtained with these studies may be helpful in understanding the electrical nature of the membrane-permeant interface [14].

2. Experimental
2.1 Materials
The experimental study was done by using cellulose acetate membrane. Cellulose acetate membrane (Cat No -190025R) used in this study was procured from Axiva Sichem Biotech, New Delhi and it was fitted in the experimental cell for study. Al (NO3)3.9H2O (SDFCL, Hyderabad) was used as such without further purification to prepare aqueous solutions using doubly distilled water. Aqueous solutions of this salt in the concentration range of 10-4 M to 10-3 M were used as permeants during measurements.

2.2 Scanning electron microscopy (SEM) analysis of the membrane

The microstructures of the membranes were studied using scanning electron microscope (Model - QUANTA 200 F) before fixing it in the experimental cell. Images of cellulose acetate membrane were taken at different magnification range as shown in Figure 1 (a & b), for viewing the surface morphology and pore size distribution.

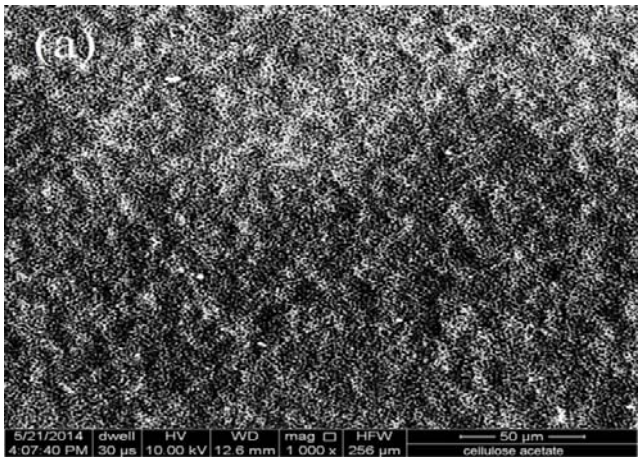

Fig 1: (a) 1,000

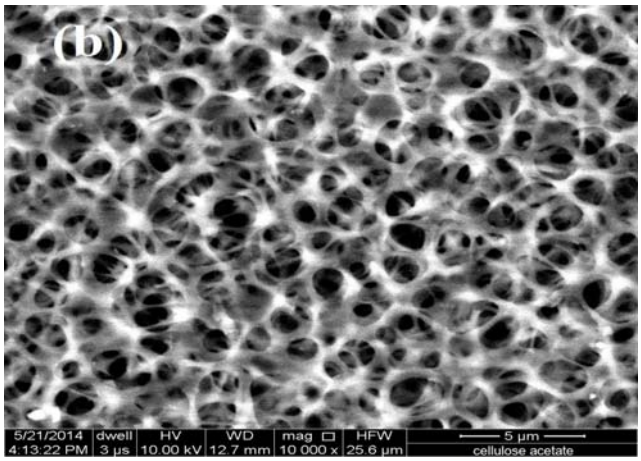

Fig 1: (b) 10,000

Fig 1: SEM images of the top surface area at different magnification:

2.3 Measurement of hydrodynamic permeability

Hydrodynamic permeability was measured by using an experimental setup, already described by many workers [14, 15]. The experimental cell was filled with the liquid under investigation, and left as such for 10 to 12 hours for equilibration before use. For maintaining the equilibrium, the cell was subsequently filled with a degassed fresh solution to confirm that the concentration of the experimental solution remained the same on both sides of the membrane. The volume flux across membrane under various pressure differences was measured by monitoring the movement of liquid-air meniscus in a horizontally placed graduated capillary tube with a cross sectional area of 7.86×10^{-7} m^2. The values of transport coefficients (L_{11}/T) determined from the data on permeability measurement are recorded in the Table.

2.4 Measurement of electro-osmotic permeability

Electro-osmotic permeability was measured by the same experimental cell as described above. Pt-electrodes were fitted in the experimental cell in such a way as to touch the membrane from both the sides. Potential differences in the range of 10 to 50 V were applied across the membrane through electrodes with the help of an electronically operated power supply (Medox-Bio, Power Supply 300 Advanced). The volumetric flux was measured by following the rate of displacement of the liquid-air meniscus in a horizontally placed graduated capillary tube with a cross sectional area of 7.86×10^{-7} m^2. The values of electro-osmotic transport coefficients (L_{12}/T) determined from the permeability measurement data are recorded in the Table. All experiments were carried out in air thermostat maintained at 30 ± 0.5^{o} C.

2.5 Measurement of Streaming current

Streaming current generated during the transport of permeants by application of various pressure differences on the two sides of the membrane were measured with a Digital Picoammeter (Model PM-100, Raman Scientific Instruments, Roorkee, India) by the technique described elsewhere [15]. The streaming current at lower pressure could not be measured correctly due to less sensitivity of the instrument. The values of transport coefficients (L_{21}/T) determined from the streaming current measurement data are recorded in the Table.

2.6 Measurement of membrane conductance

The conductivity of membrane equilibrated with permeants (L_{22}/T) and specific conductance (χ) of permeants were measured with the help of conductivity meter (Systronics-304, cell constant 1± 0.1). The values of membrane conductance and specific conductance were found to be in increasing order due to increasing concentrations of the solution and are recorded in the Table.

2.7 Measurement of viscosity of permeants

The values of viscosity are recorded and are shown in the Table. Ostwald viscometer was used for determining the viscosity (η) of each solution.

$$\eta_1 = \eta_2 \times \frac{t_1 d_1}{t_2 d_2}$$

Where, η_1 is viscosity of aqueous solutions and η_2 is viscosity of conductivity water.

t_1 is time of flow of aqueous solutions and t_2 is time of flow of conductivity water.

d_1 is density of aqueous solutions and d_2 is density of conductivity water.

3. Results and Discussion

Non-equilibrium thermodynamic theory [16] shows that volume flux, $J_{v,}$ and electrical current, I, under the simultaneous action of pressure difference (ΔP) and electrical potential difference ($\Delta\phi$) are given by:

$$J_v = \frac{L_{11}}{T}(\Delta P) + \frac{L_{12}}{T}(\Delta\phi) \quad (1)$$

$$I = \frac{L_{21}}{T}(\Delta P) + \frac{L_{22}}{T}(\Delta\phi) \quad (2)$$

Where, I is the flow of electricity and the quantities L_{mn} (m, n = 1, 2) are called the phenomenological coefficients.

When, $\Delta\phi = 0$, Eq. (1) reduces to

$$(J_v)_{\Delta\phi=0} = \frac{L_{11}}{T}(\Delta P) \quad (3)$$

Hydrodynamic volume flux, J_v, was found to show a linear dependence on the applied pressure difference, ΔP. The plots of $(J_v)_{\Delta\phi = 0}$ against ΔP as shown in Figure 2 are straight lines.

When, $\Delta P = 0$, Eq. (1) reduces to

$$(J_v)_{\Delta P=0} = \frac{L_{12}}{T}(\Delta\phi) \quad (4)$$

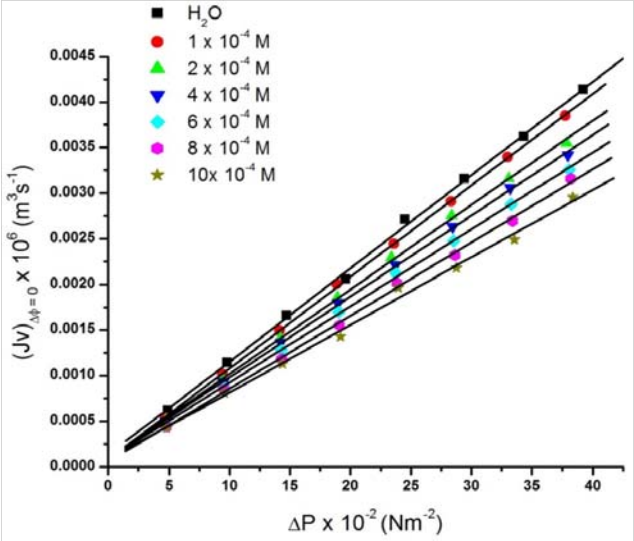

Fig 2: Hydrodynamic permeability for the Al $(NO_3)_3$-water system.

The electro-osmotic volume flux $(J_v)_{\Delta P = 0}$ against $\Delta\phi$ plots are also found linear and shown in Figure 3.

The values of phenomenological coefficients (L_{11}/ T) and (L_{12}/T), obtained from the slopes of linear plots of $(J_v)_{\Delta\phi=0}$ vs. ΔP and $(J_v)_{\Delta P = 0}$ vs. $\Delta\phi$ respectively, are recorded in the Table.

When, $\Delta\phi = 0$; Eq. (2) gives

$$(I)_{\Delta\phi=0} = \frac{L_{21}}{T}(\Delta P) \quad (5)$$

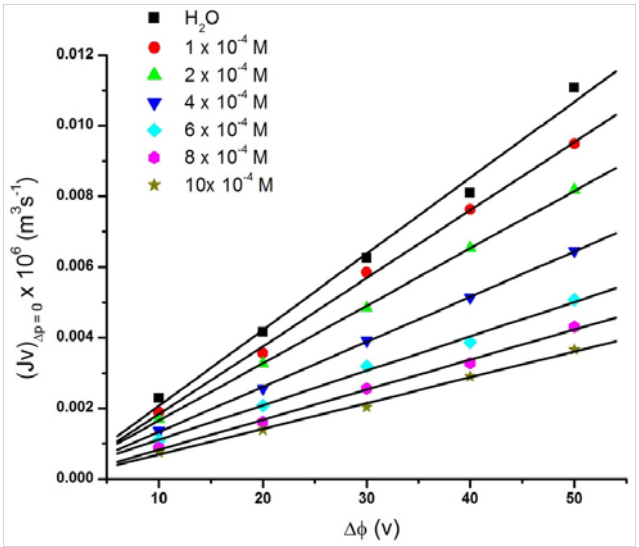

Fig 3: Electro-osmotic flux for the Al $(NO_3)_3$-water system.

Where $(I)_{\Delta\phi=0}$ is streaming current.

The plots of $(I)_{\Delta\phi = 0}$ against ΔP as shown in Figure 4 are straight lines, with slopes of giving the values of phenomenological coefficient (L_{21}/T), are recorded in the Table.

Following the theory of Overbeek [17] for the flow of liquid through single capillary; we have,

$$\frac{L_{11}}{T} = \frac{\pi r^4}{8\eta\ell} \quad (6)$$

$$\frac{L_{12}}{T} = \frac{\epsilon r^2\zeta}{4\eta\ell} \quad (7)$$

$$\frac{L_{22}}{T} = \frac{\pi r^2\chi}{\ell} \quad (8)$$

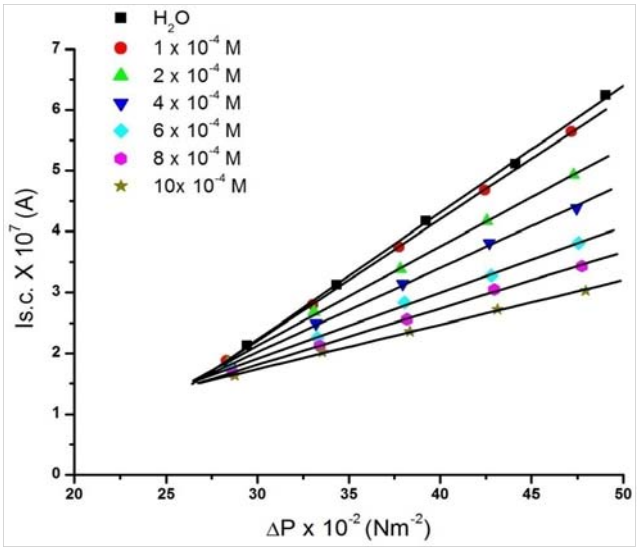

Fig 4: Streaming current flux for Al $(NO_3)_3$-water system.

If the flow occurs through a membrane which consists of parallel array of *n* capillaries, the right hand side of above equation would increase *n* times. Therefore,

$$\frac{L_{11}}{T} = \frac{n\pi r^4}{8\eta\ell} \quad (9)$$

$$\frac{L_{12}}{T} = \frac{n\epsilon r^2\zeta}{4\eta\ell} \quad (10)$$

$$\frac{L_{22}}{T} = \frac{n\pi r^2\chi}{\ell} \quad (11)$$

An examination of the table reveals that the values of L_{11}/T decreases with increase in the concentration of permeants which may be attributed to increase in viscosity of permeants. Examination of Table reveals that the values of L_{22}/T i.e. conductance of membrane- equilibrated with permeants are found in increasing order with increase in the concentration of the permeants. These results are commensurate with the conductance values of the respective solutions. Measurement on conductance of membrane-equilibrated with permeants is useful to get insight into the electro-kinetic properties of the membrane porous bodies [18] which depend on the pore size and the zeta potential of the membrane. The electrical conductivity inside the membrane may be higher than the bulk conductivity [19], these effects happen due to high salt concentrations.

In this experiment a non-ion selective CA membrane was used. During electro-osmotic flux measurements, it has been observed that flow of permeants occurred from the positive electrode to the negative electrode. This may happen due to, the electrical potential generated at the membrane-permeant interface as a result of the adsorption of hydrated anions on the membrane surface due to hydrogen bonding with first

layer of water on the membrane surface constituting Inner Helmholtz Plane (I.H.P.) and the diffused part of the double layer of the solutions constituting Outer Helmholtz Plane (O.H.P.) [20-21] contains excess of cations as shown in Figure 5. On application of electrical potential gradient, these cations flow from positive electrode to negative electrode i.e. from anode to cathode.

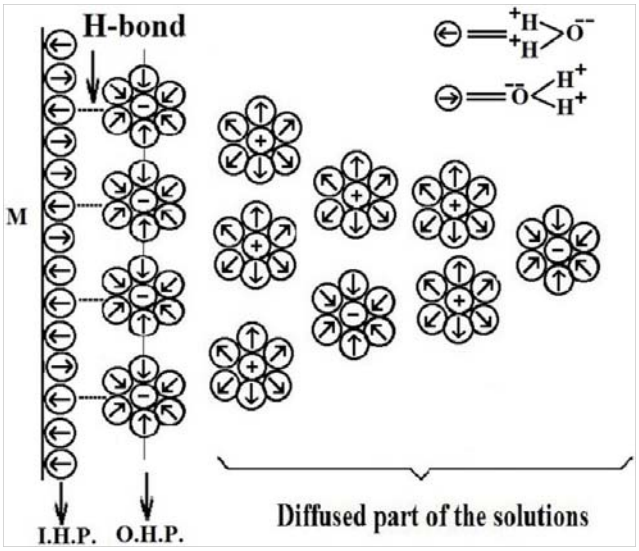

Fig 5: Postulated Picture of the electrical double layer at the nylon-66 and cellulose acetate/aqueous solution interface.
I.H.P. = Inner Helmholtz Plane
O.H.P. = Outer Helmholtz Plane
M = Membrane Surface (non-ion selective in nature)
⊕ = Cations
= ⊖ Anions

Examination of Table also reveals that the values of L_{12}/T (obtained from electro-osmotic transport equation) and L_{21}/T (obtained from streaming current measurement) are nearly equal i.e. $L_{12}/T \approx L_{21}/T$; thereby indicating the validity of Saxen's relationship.

3.1 Morphological studies of CA membrane

The microstructure of the CA membrane was characterized by Scanning Electron Microscopic (SEM) technique in different magnification range. It has been observed that at low magnification the membrane shows very small pore, granule like structure and at high magnification it shows macro pores having different pore sizes as shown in the Figure 1(a & b). In general, it is thought that morphology of the membrane having granular structure contributes to the sudden increase of solute permeability. Higher porosity of CA membranes was also responsible for the enhanced permeability property. To attain high performance of the membrane for specific applications, the morphological structures of the membranes may be manipulated.

3.2 Determination of zeta potential

Generally the zeta potentials of the membranes are supposed to represent the chemical nature of the membrane materials, which is fundamental feature and provides useful information about the electrical charge at solid-liquid surface. Evaluation of zeta potential of membranes is particularly attractive because this quantity is correlated with the mechanism of rejection of charged solutes [22]. In various solutions, electrical nature of the membrane-interfaces can be expressed in terms of zeta potential, which is estimated by combining the electro-osmotic flux coefficient (L_{12}/T) with the membrane-permeants conductance (L_{22}/T).

Zeta potentials from electro-osmotic measurements ($\zeta_{e.o.}$) were estimated from the following equation [14, 20, 21].

$$\zeta_{e.o.} = \frac{4\pi\eta\chi(L_{12}/T)}{\epsilon(L_{22}/T)} \times 9 \times 10^4 V \qquad (12)$$

Where, ϵ is the dielectric constant of the medium used, i.e. water. The values of zeta potentials estimated in this way are recorded in Table. The data for zeta potential obtained from the study on membrane indicate that it decreases with increasing concentration of solutions. The differences in the behavior of zeta potential can be explained on the basis of an altered structure of water [23] which is likely to affect the electro-osmotic behavior marginally.

Table: Phenomenological coefficients and membrane parameters for $Al(NO_3)_3.9H_2O$-aqueous system

C × 10^4 (M)	$\frac{L_{11}}{T}\times10^{13}$ ($m^5 s^{-1} N^{-1}$)	$\frac{L_{12}}{T}\times10^{10}$ ($m^3 s^{-1} V^{-1}$)	$\frac{L_{21}}{T}\times10^{10}$ ($m^{3-1} V^{-1}$)	$\frac{L_{22}}{T}\times10^{5}$ (Sm^{-1})	η×10^3 (poise)	χ ×10^5 (Sm^{-1})	$\zeta_{e.o.}$×10^3 (V)
0.0	10.21	2.15	2.13	3.90	6.08	5.07	24.012
1.0	10.02	1.93	1.99	5.40	6.10	5.63	17.344
2.0	9.25	1.62	1.64	9.50	6.23	10.40	15.612
4.0	8.87	1.27	1.37	18.20	6.37	18.59	11.676
6.0	8.39	0.97	1.08	27.00	6.51	25.00	8.262
8.0	8.01	0.85	0.91	36.00	6.67	31.70	7.054
10.0	7.40	0.73	0.73	44.00	6.80	39.10	6.217

4. Conclusion

Sorption takes place in the membrane matrix due to accumulation of electrolyte ions in membranes. Thermodynamic theory of irreversible processes confirms the validity of the linear phenomenological relations, and zeta potential values indicate the existence of electrical charge on membrane surface which also gives information about the net charge on the surface as well as the charge distribution inside the electric double layer (EDL). The SEM analysis also confirms that CA membrane having different sizes of small pores and fine surface morphology may be useful for numerous purposes in separation areas also. Sometimes evolution of gases occurs at the electrodes due to polarization which may occur when higher electrical potentials are applied across the electrodes; this was, however, minimized by using freshly boiled conductivity water for filling the apparatus.

Acknowledgments
Authors would like to thank Banaras Hindu University, Varanasi, for the laboratory facilities and University Grant Commission, New Delhi, for financial support as Rajiv Gandhi National Fellowship. We also thanks, to the Department of Metallurgical Engineering IIT-BHU, Varanasi for SEM analysis of the membrane.

List of symbols
J_v Volume flux (m^3s^{-1})
L_{11} Phenomenological coefficient representing hydrodynamic permeability ($m^5 s^{-1} N^{-1}$)
L_{12} Phenomenological coefficient representing electro-osmotic permeability ($m^3 s^{-1} V^{-1}$)
L_{21} Phenomenological coefficient representing streaming potential ($m^3 s^{-1} V^{-1}$)
L_{22} Phenomenological coefficient representing conductivity of the membrane-permeant system (Sm^{-1})
ΔP Pressure difference (Nm^{-2})
I Electric current (A)
C Concentration (M)

Greek symbols
ϵ Dielectric constant of the medium
$\zeta_{e.o.}$ Zeta potential calculated from electro-osmotic flux data
η Viscosity coefficient (Poise)
χ Specific conductance (Sm^{-1})
$\Delta\phi$ Electrical Potential difference (V)

References
1. T. Mohammadi, E. Saljoughi, Effect of production conditions on morphology and permeability of asymmetric cellulose acetate membranes, Desalination 243 (2009) 1-7.
2. M. Sivakumar, D. R. Mohan, R. Rangarajan, Studies on cellulose acetate-polysulfone ultrafiltration membranes II. Effect of additive concentration, J. Membrane Sci. 268 (2006) 208-219.
3. J. B. Jensen, T. S. Sorensen, B. Malmgren-Hansen, P. Sloth, Ion-exchange and membrane-potentials in cellulose-acetate membranes separating solutions of mixed electrolytes, J. Colloid Interface Sci. 108 (1985) 18-30.
4. K. Singh, A. K. Tiwari, Studies on the electrochemical characterization of cellulose acetate and dowex-50 membranes for uni-univalent electrolytes in aqueous solutions, J. Colloid Interface Sci. 210 (1999) 241-250.
5. K. Singh, A. K. Tiwari, C. S. Dwivedi, Electrochemical studies on surfactant-modified cellulose acetate membrane, J. Colloid Interface Sci. 266 (2003) 403-406.
6. E. Saljoughi, M. Sadrzadeh, T. Mohammadi, Effect of preparation variables on morphology and pure water permeation flux through asymmetric cellulose acetate membranes, J. Membrane Sci. 326 (2009) 627-634.
7. J. J. Qin, Y. Li, L. S. Lee, H. Lee, Cellulose acetate hollow fiber ultrafiltration membranes madefrom CA/PVP-360K/NMP/water, J. Membrane Sci. 218 (2003) 173-183.
8. I. Prigogine, Introduction to thermodynamics of irreversible processes, 2nd revised edn. Interscience, New York, 1961.
9. K. G. Denbigh, Thermodynamics of steady state, Wiley, New York, 1951.
10. S. R. de Groot, Thermodynamics of irreversible processes, North-Holland, Amsterdam, 1952.
11. R. P. Rastogi, R. C. Srivastava, P. Chand, Membrane oscillations involving electrokinetic phenomena, J. Colloid Interface Sci. 263 (2003) 223-227.
12. R. P. Rastogi, R. C. Srivastava, S. N. Singh, Nonequilibrium thermodynamics of electrokinetic phenomena, Chem. Rev. 93 (1993) 1945-1990.
13. R. P. Rastogi, R. C. Srivastava, Interface-mediated oscillatory phenomena, Adv. Colloid Interface Sci. 93 (2001) 1-75.
14. M. L. Srivastava, B. Ram, Electrokinetic studies of the testosterone- aqueous d-glucose interface, Carbohydr. Res. 132 (1984) 209-220.
15. M. L. Srivastava, B. Ram, Electrokinetic studies on testosterone/aqueous electrolyte interface: Part 1. Electro-osmosis, electrophoresis, streaming potential and streaming current. J. Membrane Sci. 19 (1984) 137-153.
16. A. Katchalsky, P. F. Curran, Non-equilibrium Thermodynamics in Biophysics, Harvard University Press, Cambridge, MA, 1965.
17. J. T. G. Overbeek, H. R.Kruyt, Ed., Colloid Science 1, Elsevier, Amsterdam & New York, 1952.
18. A. E. Yaroshchuk, T. Luxbacher, Interpretation of electrokinetic measurements with porous films: role of electric conductance and streaming current within porous structure, Langmuir 26 (2010) 10882-10889.
19. A. Szymczyk, P. Fievet, B. Aoubiza, C. Simon, J. Pagetti, An application of the space charge model to the electrolyte conductivity inside a charged microporous membrane, J. Membrane Sci. 161 (1999) 275-285.
20. R. Shabd, B.M. Upadhyay, Electrokinetic studies on carbohydrates, Carbohydr, Res. 90 (1981) 187-192.
21. R. Shabd, B.M. Upadhyay, Electrokinetic studies on cholesterol-carbohydrate systems, Carbohydr. Res. 93 (1981) 191-196.
22. C. Labbez, P. Fievet, F. Thomas, A. Szymczyk, A. Vidonne, A. Foissy, P. Pagetti, Evaluation of the "DSPM" model on a titania membrane: measurements of charged and uncharged solute retention, electrokinetic charge, pore size, and water permeability, J. Colloid Interface Sci. 262 (2003) 200-211.
23. R. E. Kesting, Synthetic Polymeric Membranes, McGraw-Hill, New York, 1971.